



# Advanced Diffraction and Scattering

---

*Beamline Scoping Group Report*

Dr John Daniels (UNSW)  
Dr Matthew Rowles (CSIRO)  
Dr Klaus-Dieter Liss (ANSTO)  
Prof. Richard Welberry (ANU)  
Dr Justin Kimpton (AS)  
Dr Kia Wallwork (AS)

*31-8-2011*

---

# Contents

|  |    |
|--|----|
| Introduction .....   | 3  |
| High-energy x-ray scattering.....                                    | 4  |
| Complementarity with existing and proposed beamlines at the AS ..... | 5  |
| Complementarity with OPAL neutron scattering facilities .....        | 6  |
| ADS experimental configurations .....                                | 6  |
| Monochromatic scattering .....                                       | 6  |
| High quality .....   | 6  |
| High acquisition rate .....  | 7  |
| Side hutch .....   | 7  |
| Polychromatic scattering .....                                       | 7  |
| Energy dispersive diffraction .....                                  | 8  |
| White beam Laue diffraction .....                                    | 8  |
| Imaging.....   | 8  |
| Advanced techniques.....   | 9  |
| Industrial access.....   | 9  |
| Critical beam parameters.....  | 9  |
| Proposed beamline .....  | 10 |
| Schematic layout.....  | 10 |
| Alternate layout .....   | 10 |
| Critical components .....  | 11 |
| Source .....   | 11 |
| Front-end aperture .....   | 11 |
| Filters and windows .....  | 11 |
| Primary slits.....   | 12 |
| Transfocator.....  | 12 |
| Side-bounce monochromator.....                                       | 12 |
| Monochromator tank 1.....  | 13 |
| Mirror tank.....   | 14 |
| Monochromator tank 2.....  | 14 |
| Secondary slits .....  | 14 |
| Experimental hutches .....   | 14 |
| Sample environments .....  | 15 |
| Detectors.....   | 16 |
| Large area high quality.....   | 16 |
| Large area rapid acquisition.....                                    | 17 |

|   |    |
|---|----|
| Multi-element energy resolving.....   | 17 |
| Imaging.....  | 17 |
| Beamline control systems.....   | 18 |
| Beamline control cabins.....  | 18 |
| Commercial data analysis software and licenses .....  | 18 |
| Laboratory infrastructure .....   | 18 |
| Solid sample preparation .....  | 18 |
| Chemistry .....   | 18 |
| Experimental preparation .....  | 18 |
| Data transfer requirements .....  | 19 |
| Preliminary costings.....   | 19 |
| Non-critical components.....  | 20 |
| Conceptual design.....  | 20 |
| Similar beamlines.....  | 21 |
| Example studies .....   | 23 |
| Total scattering analysis.....  | 23 |
| Negative thermal expansion materials - Kepert, University of Sydney .....                     | 23 |
| Atomic anisotropy of thermal expansion in bulk metallic glass –Liss, ANSTO .....              | 24 |
| Single crystal diffuse scattering .....   | 24 |
| Relaxor ferroelectrics and other functional oxide ceramics - Welberry, ANU .....              | 24 |
| Materials mapping and texture analysis.....   | 25 |
| Study of residual strain in thermal barrier coatings - Thornton, DSTO .....                   | 25 |
| Phase transitions in metal alloys - Liss, ANSTO.....  | 26 |
| 2D mapping of strain distributions in Zr-hydrides – Daniels, UNSW .....                       | 27 |
| Energy dispersive diffraction .....   | 27 |
| Passivation layers in inert anodes - Rowles, CSIRO .....                                      | 27 |
| International studies.....  | 28 |
| Strain in amorphous materials - Poulsen, Risø National Laboratory .....                       | 28 |
| Combined X-ray diffraction and imaging - Ludwig, ESRF .....                                   | 29 |
| Anomalous diffraction at ultra-high energy for protein crystallography - Jakoncic.....        | 29 |
| 3D Grain mapping by toptotomography - Ludwig, ESRF .....                                      | 30 |
| Uniaxial stress at high temperature and pressure - Grima Gallardo, Universidad de Los Andes.  | 30 |
| X-ray diffraction contrast tomography - Ludwig, ESRF & Johnson, University of Manchester .... | 30 |
| References .....  | 31 |

## Introduction

The Advanced Diffraction and Scattering beamline outlined here will provide a unique range of experimental opportunities for both fundamental and applied scientific research. The proposed beamline fills an important gap in Australian research infrastructure and will play a key role in allowing Australian researchers to access a full range of world class characterization facilities. Much of the research performed on comparable beamlines around the world falls directly into Australia's National Research priorities. In particular, the development of advanced materials for the energy sector, manufacturing technique development and optimisation, and minerals processing are common applications of this unique tool.

The proposed beamline will provide opportunities for scientists to explore problems using a broad range of experimental techniques which include, but are not limited to,

- 1) Rapid 'traditional' powder diffraction using complex *in-situ* sample environments
- 2) Total scattering analysis or Pair Distribution Function (PDF) analysis of crystalline and amorphous materials
- 3) Diffuse scattering studies of single crystals for structural and charge density analyses
- 4) Rapid texture analysis, 3-dimensional reciprocal space, and 2-dimensional materials mapping
- 5) Scanning diffraction tomography
- 6) Low-dose protein crystallography
- 7) Energy dispersive diffraction studies from isolated 3-dimensional gauge volumes
- 8) High resolution 3-dimensional strain scanning of large volume materials
- 9) White/Pink beam Laue diffraction
- 10) High speed imaging
- 11) Combined imaging and scanning diffraction for multi-length scale studies

Currently, Australian research groups make use of available high energy x-ray sources worldwide to carry out such experiments. This work is primarily performed at the worlds three major high energy storage rings; the European Synchrotron Radiation Facility, France, the Advanced Photon Source, USA, and Spring 8, Japan. The beamtime available at these sources is limited and proposal review processes are highly competitive, restricting Australian access. As an example, beamline ID15 of the ESRF has operated with a consistent over-subscription rate of 3-5 for the past 5 years, while the high-energy materials beamline at Petra III has become the facilities most oversubscribed beamline in the first year of operation [1]. Larger facilities have recognised the increasing demand for high-energy x-rays and are accommodating it where possible. Under the ESRF upgrade program, for example, an additional dedicated materials science beamline operating at energies above 30 keV will be added to the facility (UPBL II) [2].

While Australian access to these higher-energy storage rings is limited, there is a strong user community within this country, as shown by the number of applications to the International Synchrotron Access Program (ISAP) for successful beamtime proposals at these facilities. Over the past 2 years, a total of 21 applications have been made to ISAP for the use of high-energy x-rays [3]. Noting the oversubscription rate of the beamlines, and relatively low success rate of beamtime proposals at these facilities, this number represents a significant Australian research body with great interest in performing high-energy x-ray experiments. The present authors are also regularly approached by an even larger community that would like to apply high-energy x-ray scattering techniques to their own projects, however, in most cases this has to be turned down for reasons of availability and resources. Furthermore, the complementarity to neutron scattering techniques, in which Australia has a large and vibrant user community, will provide an ever increasing user base.

We believe this is strong evidence that such a beamline will immediately become oversubscribed by the Australian user community performing high-quality scientific experiments.

Traditionally, higher energy storage rings were the only machines capable of producing high brilliance x-ray beams with energies above 50 keV. Recent advances in insertion device technology however, namely high-field superconducting wigglers, have allowed lower energy storage rings such as 3 GeV machines to produce high energy x-ray beams of comparable quality. Beamline I12 of the Diamond light source has been the first dedicated high-energy source at a 3 GeV storage ring with a particular emphasis on hard condensed matter and materials research. This beamline has also experienced an oversubscription rate >2 in its first year of operation [4]. Other low energy storage rings, such as NSLS-II and Soleil, are now moving towards installing superconducting wigglers or similar devices to allow for x-ray scattering experiments above 30 keV.

### High-energy x-ray scattering

High-energy synchrotron x-ray scattering is a powerful tool for materials characterization over many length scales [5]. While conventional x-ray diffraction techniques are generally surface sensitive, high-energy x-ray scattering is a true bulk materials analysis method. Figure 1 displays the transmission of x-rays through 1 mm of selected material types as a function of photon energy. It can be seen that as energies well above 30 keV are reached, even higher atomic number materials, such as Sn and Pb, are penetrated allowing scattering information to be collected in transmission geometries from bulk samples.

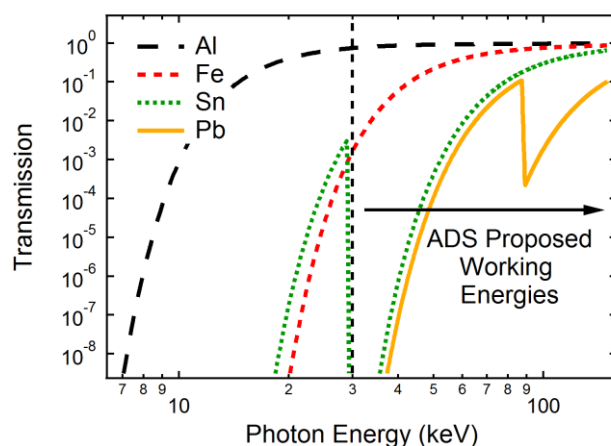


Figure 1. Transmission of x-rays through 1mm of selected materials as a function of photon energy. Working energies of proposed ADS beamline indicated above 30 keV.

The high-energies also result in low scattering angles and accessibility of high momentum transfer ( $q$ ) information, providing several advantages. For regular monochromatic diffraction experiments, sample environments can operate with very small windows for both the entrance and exit beams. Coupled with the penetrating power, this results in the possibility to perform in-situ experiments in highly complex sample environments such as cryogenic magnets, thermo-mechanical testing instruments, reaction chambers, and pressure cells. The possibility to then access high  $q$ -vector information is also realised. Figure 2 shows the scattering angle ( $2\theta$ ) experimental space which needs to be covered in order to collect scattering data to a  $q$ -vector magnitude of  $30 \text{ \AA}^{-1}$  (a typical value required for high-quality Pair Distribution Function (PDF) analysis). This Figure highlights the fact that this cannot be achieved with energies below 30 keV even with a full sphere of  $2\theta$  detector coverage. Also indicated is that at 100 keV, this  $q$ -range can be achieved relatively easily with a large area detector at a typical sample to detector working distance of approximately 250mm (calculated for a  $400 \times 400 \text{ mm}^2$  detector and max  $2\theta$  of  $35^\circ$ ).

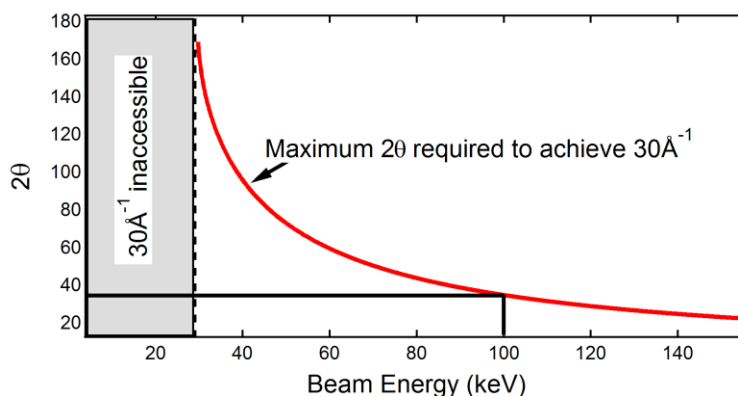


Figure 2.  $2\theta$  required to access  $q$ -space to a scattering vector magnitude of  $30 \text{ \AA}^{-1}$ . The shaded area represents energies at which this is impossible, while the solid line shows how at 100 keV this is easily achieved.

One of the most powerful features of high-energy x-ray scattering techniques is realised when conducting experiments where a vector field is applied to the sample, such as an applied mechanical load, electric or magnetic field, etc. Monochromatic high-energy x-ray scattering with a large area detector, or polychromatic scattering with multi-element energy dispersive detector, allows one to collect diffraction information with the scattering vector aligned at various angles to this applied field simultaneously. The scattering vector cone, shown in Figure 3, represents the possible scattering vector orientations sampled simultaneously in the 2D image of a monochromatic diffraction pattern. One face of the cone is a flat surface lying exactly perpendicular to the beam direction and the opening of the scattering vector cone is  $2\theta_{\text{max}}/2$  (generally  $<5^\circ$  at 90 keV photon energy). Thus, when a vector field is applied perpendicular to the beam, scattering information marked in Figure 3 (a) can be separated into its angle from this applied field. This is a feature unique to high-energy x-ray and spallation neutron sources, and is critical to understanding many physical processes occurring in materials under the application of vector fields. At present the Australian user community does not have local access to either of these facilities, thus the proposed beamline fills this important gap in the current research infrastructure.

Utilising energy-dispersive diffraction techniques with suitable slit systems at high x-ray energies also allows the isolation of scattering information from a fixed 3D gauge volume in sample space. Such a possibility is usually only achieved using neutron scattering techniques, however, the gauge volumes possible with x-ray scattering are generally 1-2 orders of magnitude smaller than with neutrons, allowing for greater spatial resolution [6]. In addition, the speed of data acquisition is dramatically increased over the neutron scattering equivalent. This technique has primarily been used for 3D strain scanning of engineering components, however, it is now finding increasing application in *in situ* diffraction studies where it is necessary to eliminate scattering from sample environments, such as battery and fuel cell research [7].

### Complementarity with existing and proposed beamlines at the AS

At extreme points of its operational parameters, the capabilities of the proposed ADS beamline overlaps with powder diffraction (PD), imaging and medical beamline (IMBL), and the proposed micro-CT beamlines. In order to maintain maximum complementarity with the existing Powder Diffraction beamline, the ADS beamline will provide a useable x-ray flux at 30 keV (the lowest energy available at the ADS), giving access to a continuous X-ray spectrum from 4 keV to 150 keV across the two beamlines. The ADS imaging capabilities will be differentiated from the IMBL in the provision of; 1) rapid focused white-beam imaging and, 2) combined diffraction/imaging experiments to provide complementary information about the microstructure and crystallinity of materials. Finally, due to the minimal overlap in incident energies, the imaging capabilities of the ADS and micro-CT beamlines will be able to provide complementary information.

## Complementarity with OPAL neutron scattering facilities

The ADS beamline will fill an important gap between the current x-ray scattering facilities at the Australian Synchrotron, and neutron scattering facilities at the Australian Nuclear Science and Technology Organisations OPAL research reactor. The two techniques can be used in combination to probe bulk solid materials from the level of single grains (high energy x-rays) to averaging volumes of the order of several  $\text{cm}^3$  (neutron powder diffraction). It is also often advantageous to have scattering information using both neutrons and x-rays, as the differences in relative scattering lengths can be used for more accurate structural analysis. However, the transfer of samples, and sample environments, from neutron to synchrotron x-ray experiments requires significant effort and is often inhibitive to successful collection of such complementary data sets. High energy x-ray scattering fills this gap by allowing similar sample geometries and sample environments to be used for both experimental techniques. Similarly, users who find high-energy x-ray scattering techniques of use to their applications can also in many cases use neutron scattering facilities for additional information, such as sensitivity to light elements, isotopic contrast, and magnetic studies.

## ADS experimental configurations

The beamline will be configurable in several ways to take full advantage of the proposed superconducting wiggler source. These will be,

- 1) Monochromatic Scattering
  - a. High quality
  - b. High intensity
  - c. Side hutch
- 2) Polychromatic Scattering
- 3) Imaging

## Monochromatic scattering

Figure 3 shows several of the most common monochromatic scattering techniques used. Here, conventional powder diffraction, high-q total scattering (for PDF analysis), single crystal diffuse scattering, high-q amorphous material scattering (for PDF analysis), and single crystal scattering are shown in Figure 3 (a) to (e), respectively. Each of these techniques uses a similar setup within the experimental end station with the only variable parameters being the sample environment and sample to detector distance. It should be noted that such a simple experimental setup is also not limited to only these techniques. Other advanced techniques such as 3-dimensional x-ray diffraction (3DXRD) [8] will use the same setup. The optimum beam optics for each experiment, however, may vary depending on the type of experiment performed. For example, amorphous PDF and diffuse scattering studies generally do not require high q-resolution, however, they are often flux limited, thus, broad bandwidth focussing monochromators can be used to maximise incident beam flux. On the other hand, strain measurements from metallic materials require the highest possible peak position resolution, here Rowland geometry monochromators optimise the beam quality but sacrifice flux at the sample.

### High quality

Utilising a transfocator system [9] with double Laue monochromators in Rowland geometry, a versatile spot size and bandwidth of the incident beam is achieved. The beam, in this case, is highly symmetric and can be used for medium to high resolution powder diffraction and strain scanning techniques. This configuration, however, results in a significant loss in flux of the incident beam due to the small acceptance aperture of the compound refractive lenses of the transfocator (typically  $1 \times 1 \text{ mm}^2$  maximum). The advent of the transfocator operating as close as possible to the source has minimised these losses and the expected beam intensity at the sample in this configuration would

be estimated to significantly exceed that of the I12 beamline at Diamond as they do not currently operate with such a system.

The achievable spot size using compound refractive lenses is proportional to the ratio of distances from the source-lens and lens-sample, analogous to optical systems. Therefore, a second set of lenses closer to the sample can dramatically reduce the achievable spot size and allow for micro-focussing of high-quality monochromatic beams.

### High acquisition rate

Using a focussing monochromator system, a very large portion of the incident beam fan can be focussed to the sample area, dramatically increasing the monochromatic flux. Such focussing geometries, however, introduce energy gradients through the beam, and thus subtle asymmetries into measured data. On the other hand, high-flux monochromatic beams offer the ability to improve the time resolution of single shot diffraction experiments well below 1 ms. This technique would also be used for low resolution experiments that require the maximum possible flux, such as total scattering and diffuse scattering methods.

### Side hutch

Monochromatic scattering will also be possible in an experimental side hutch which can be operated simultaneously to the main hutch. It has been proven at existing facilities that a large amount of high quality work can be performed in parallel with the main station and the user access doubled for a relatively small additional cost on the X-ray beam delivery. The proposed high energy beamline is expected to be significantly oversubscribed, thus, we strongly recommend setting up such a side station.

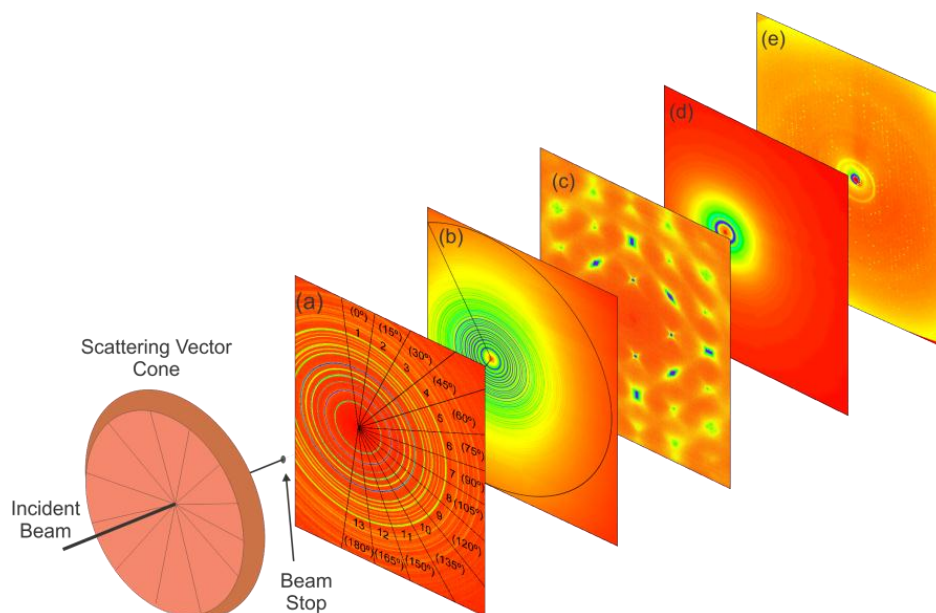


Figure 3. Schematic diagram showing the typical scattering patterns recorded for various experiments. (a) regular powder diffraction from polycrystalline materials, (b) powder diffraction data measured to high-q values for pair-distribution function analysis, (c) single crystal diffuse scattering, (d) liquid and amorphous material scattering measured to high-q, (e) single crystal Bragg scattering. The scattering vector cone represents the angles at which all possible scattering vectors lie.

### Polychromatic scattering

Both polychromatic techniques outlined below will use the same experimental optics configuration, either a slitted down, or mirror-focussed, white beam of the order of 10-1000 $\mu$ m.

### Energy dispersive diffraction

This technique is primarily used for high resolution 3D strain scanning of large components, however, it is increasing used for complex in-situ experiments such as investigating the operation of electro-winning cells, fuel cells, and batteries [7]. Gauge volumes are generally in the range of 10-100  $\mu\text{m}$  in diameter, but can be up to 1 mm, and are elongated along the beam direction. By increasing the number and orientation variance of the receiving detectors, this technique can typically provide good quality diffraction and orientation information on a time scale of  $< 10$  s. This experimental setup requires the accurate positioning of a tungsten slit system between the sample and the detector.

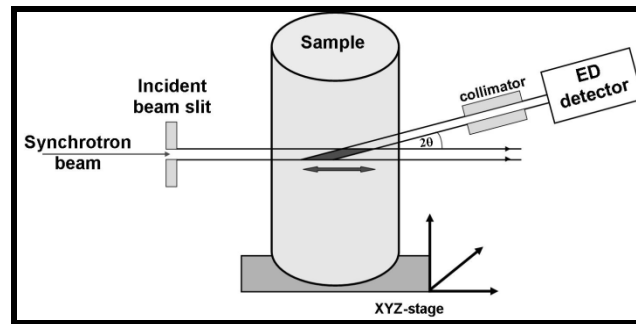


Figure 4. Experimental setup for polychromatic scattering experiments where a gauge volume can be isolated in 3 dimensions.

### White beam Laue diffraction

White beam Laue diffraction techniques offer the ability to rapidly characterise crystal structures. At high x-ray energies the scattering information is constrained in the forward direction, thus, coupled with suitable area detectors the possibility exists for single or multi crystal studies with time resolutions below 10 ms. At the forefront of this technology, white beam Laue diffraction is being applied to illuminating a small number of crystallites embedded in polycrystalline materials while external load is applied to the sample. It allows one to determine orientation gradients, crystallite quality, transformations and deviatoric strains simultaneously.

### Imaging

The imaging configurations of the beamline will be limited since the IMBL will have a similar source and therefore should be capable of performing the same imaging applications. However, in state-of-the-art studies, diffraction and imaging should not be totally separated and thus, there are possible exceptions to this,

- 1) When imaging is combined with scanning beam scattering. Here the radiographic and/or tomographic images are required for complementary information during in-situ experiments or to align a particular feature of interest for scattering experiments.
- 2) The proposed broad bandwidth beams generated by the transfocator or possible white beam mirrors will provide significant intensity increases over other high-energy imaging beamlines. The possibility to perform medium resolution rapid micro-tomography using CMOS detectors will exist.

It should be noted, however, that the possibility for additional imaging capabilities in the future will always exist. Minor alterations to the proposed monochromator systems would be required for similar high quality imaging as that performed at the IMBL. This will depend on future demand for the IMBL and ADS beamline for high-energy imaging.

## Advanced techniques

The beamline also offers the opportunity for groups with interest in technique development to take advantage of a unique high-energy x-ray source. This is especially necessary to address the ever growing opportunities based on new detector and computing developments, and to keep the beamline competitive on a world level. In order to accommodate this, we propose to leave several free stages within the optics system for the later addition of newly developed optics components. This will consist of a single versatile stage within each of the proposed monochromator tanks and a possible free section within the transfocator. Such accommodations at the period of design and construction dramatically reduce the time, cost, and experimental complexity of these developments in the future.

## Industrial access

Industrial access to high-energy x-ray scattering beamlines is relatively high. Of particular interest is the ability to perform high spatial resolution strain scanning in 3D. Residual stresses generated during manufacturing limit component lifetime, thus commercial users are often interested in comparing stress fields from components manufactured in various ways prior to full scale production. There is the potential to market this application to south-east Asian manufacturing industries. ID15 of the ESRF has successfully marketed strain scanning beamtime to major industries in Europe, in particular Airbus Industries and Rolls Royce. Typical rates for commercial access are of the order of €5000/8 hour shift. I12 of Diamond light source also plans to perform commercial strain scanning experiments using energy dispersive diffraction.

As well as strain scanning, there is also the possibility to market the rapid in-situ techniques to chemical processing and thermo-mechanical processing industries. The unparalleled speed of diffraction data acquisition combined with high-quality in-situ sample environments could provide a unique method for industries to streamline processing conditions. The acquisition of an industrial standard in-situ testing instrument will be critical to commercial up-take of such techniques. The thermo-mechanical deformation instrument proposed below (Gleeble) fits this requirement and to our knowledge, no such industrial standard instrument exists on other high-energy scattering beamlines.

## Critical beam parameters

The table below shows some of the critical beam parameters which the ADS beamline will achieve with the proposed experimental layouts. It should also be noted that the facility for the expansion of these parameters is a primary design requirement as techniques and instrumentation in the field evolve.

| Configuration                                 | Main Hutch                 |                              | Side Hutch           |                              |
|---|----------------------------|------------------------------|----------------------|------------------------------|
|   | High Quality Monochromatic | High Intensity Monochromatic | White beam           | Medium Quality Monochromatic |
| Energy Range (keV)                            | 30-150                     | 30-150                       | 30-maximum available | Discrete energies 30-100     |
| Bandwidth (eV)                                | 50-300                     | ~300 including gradient      |                      | ~300                         |
| Focused Spot Size at Sample ( $\mu\text{m}$ ) | 10-400                     | 200-1000                     | 10-500               | 100-500                      |

## Proposed beamline

### Schematic layout

Figure 5 below shows the schematic layout if the beamline design is to be restricted to the footprint of the experimental hall (we highlight the possibility of extending the beamline in a subsequent section below). The critical components are colour coded to represent the type of beamline operation they are designed for. This layout will be capable of operating two high-energy end stations simultaneously. The monochromatic side station beam is generated by a single monochromator which is transparent and allows the white beam to continue to the main experimental hutch. Here, the operation of the side station is limited to a diffraction angle of approximately  $10^\circ$  from its monochromator. This angle is critical to the energy range and intensity available in the side station.

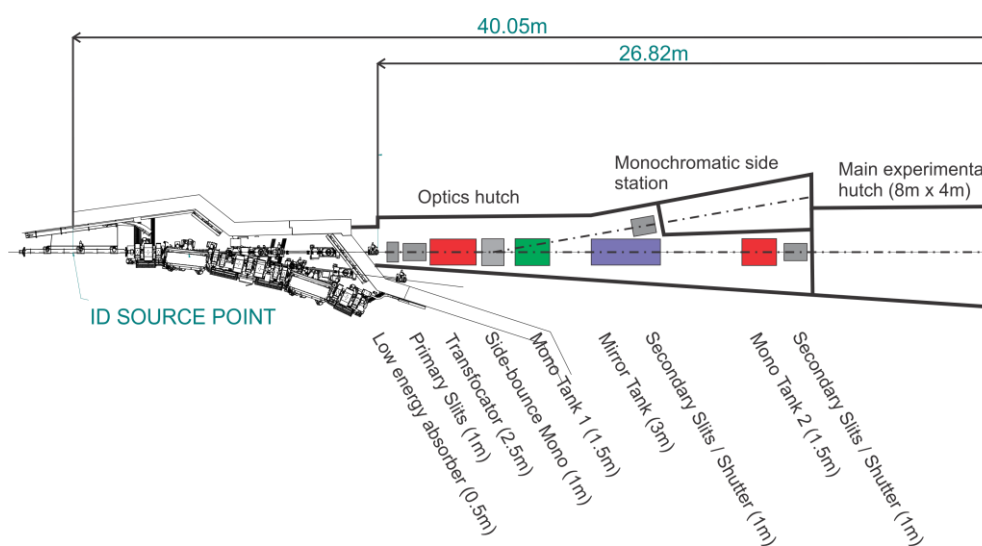


Figure 5. Schematic layout of proposed ADS beamline. Grey components are in use for all possible beamline configurations. Red components are in use for high-quality monochromatic scattering. Green components are in use for high-intensity monochromatic scattering. And purple components are in use for high-intensity polychromatic scattering.

### Alternate layout

In order to obtain the best performance from this beamline, it would be preferential to extend the beamline by 10 – 30 m beyond the current experimental floor footprint. A schematic of the possible layout of this extended version of the proposed ADS is shown in Figure 6. Here, the main experimental hutch is moved a further 20 meters from the source. All critical components of the beamline and the experimental hutch layouts would be identical to that proposed above. It is estimated that the beamline performance would be significantly improved in several ways;

- 1) The monochromator angle to the side hutch could be reduced from  $10^\circ$  to  $5^\circ$  in order to obtain higher flux at higher energies into the side station by using lower order monochromator reflections (see Side-bound Monochromator section below).
- 2) The number of compound refractive lenses used for the high-quality monochromatic mode in the main hutch could be reduced, thus increasing the flux for this operational setup by reducing absorption in the lenses.
- 3) Using secondary sets of compound refractive lenses close to the sample, the achievable spot sizes available in the main hutch could be significantly reduced. This reduction is proportional to the relative distance of the focal length of the refractive optic to the distance from the source.

- 4) The size of the main experimental hutch could be increased. Near and far-field detectors, the latter up to 7 m from the sample, would allow the study of minute features in the diffraction profile in 2D or 3D reciprocal space.

Extending the beamline will have an effect on the design and cost, as well as impacting on the number, types and positions of the experimental hutches. It is proposed that the initial step of the preliminary conceptual design will be to quantify the beamline performance at both proposed lengths.

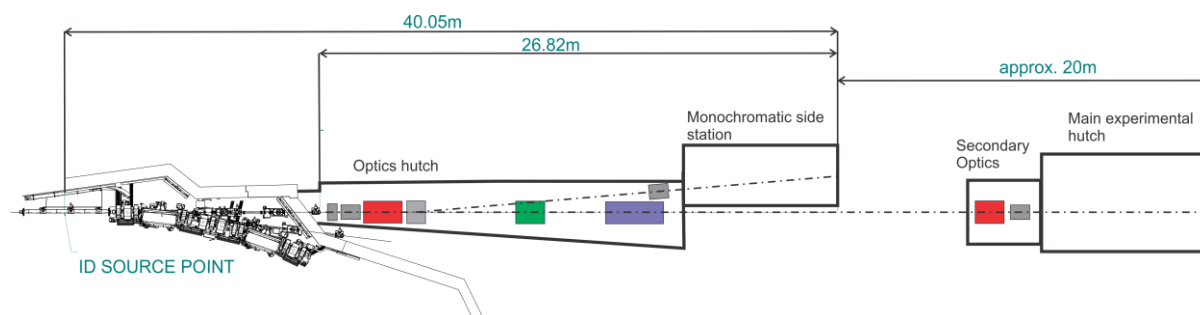


Figure 6. Schematic layout of extended version of ADS. Here, all critical components are identical to those labelled in Figure 5.

## Critical components

### Source

The source proposed is the superconducting multi-pole wiggler produced by Budka. The ADS beamline will provide x-rays over the range of 30-150 keV. In order to enable energy-dispersive and white-beam Laue diffraction techniques, as well as monochromatic diffraction and imaging techniques, the continuous output of a wiggler source is ideal. The high power of this source will impose strict requirements on beam filtering and downstream component cooling, as well as radiation shielding. Using the same or similar source to the IMBL will take advantage of the front end and heat management systems already designed for that beamline. The source will also require a helium recovery system.

### Front-end aperture

The front end aperture will decide the ultimate available beam size and focused flux of the beamline. Due to the large fan of the wiggler source it will be necessary to limit the horizontal acceptance of the beamline to limit the thermal power deposited on the upstream optics. Since the source spectrum and fan will be similar to that of the IMBL, the ADS beamline will take advantage of the front end and heat management already designed for IMBL.

A basic calculation of the beam size as a function of distance from the source is shown in Figure 7 for two horizontal aperture sizes. We propose a front end horizontal aperture of the order of 1-1.5 mrad to give the greatest versatility of the beamline applications, with lowest radiation shielding costs.

### Filters and windows

Most of the thermal power of the wiggler lies at low energies, < 30 keV. To reduce the impact of this heat load on the performance of the optical elements, this power must be reduced through the use of suitable filters and window materials. In order to maintain maximum complementarity with the existing Powder Diffraction beamline, the ADS beamline should provide a useable x-ray flux at 30 keV, giving access to a continuous x-ray spectrum from 4 keV to 150 keV across the two beamlines. In addition to the filters responsible for optical component heat management, additional filters

should be available to reduce potential radiation damage to delicate samples, as well as hardening the incident beam for white-beam imaging experiments on high-Z materials.

Typical absorber materials include CVD diamond and SiC, while beam hardening filters are generally Cu. JEEP at Diamond has fixed CVD diamond and a suite of Cu filters in a range of thicknesses from 1–8 mm, all of which are water cooled.

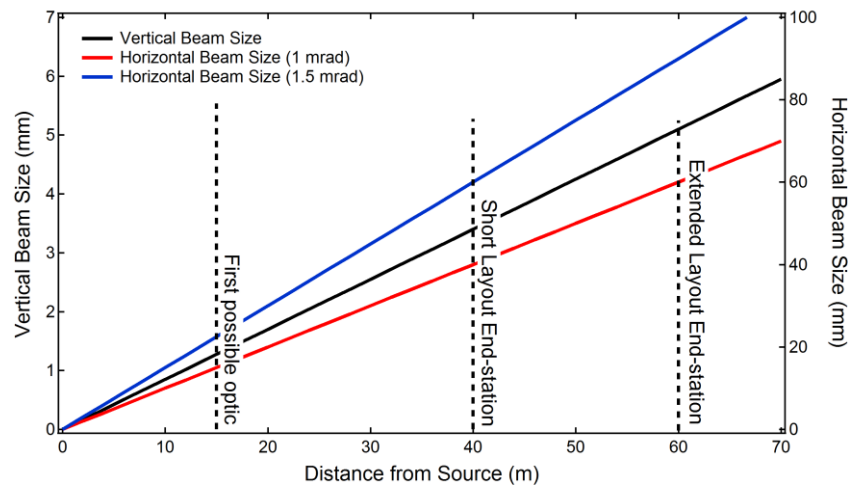


Figure 7. Approximate source fan size as a function of distance. Vertical dashed lines indicate the approximate positions of the first possible optic device (outside the front end) and the maximum possible distance.

### Primary slits

A primary slit system to vary the incident beam aperture to the remainder of the beamline is a critical component. These slits must be able to absorb the full heat load at this point. They must also be precise to set accurate beam sizes. Water cooling is usually used to keep the slits from overheating under the full beam condition. As these slits will have to operate with incident energies of up to 150 keV, the leading and trailing edges of the slits will have some appreciable transparency. The slit faces should be precisely aligned to the divergent X-ray beam to ensure that the full depth of the slit is presented to the beam at all times. Tapered tungsten slits are most commonly used. At the proposed distance from the source, the primary slits of the ADS will require 0-5 mm and 0-30 mm opening range in the vertical and horizontal directions, respectively.

### Transfocator

The transfocator device [9] has been an ESRF development and utilises pre-aligned sets of compound refractive lenses which can be combined in multiple configurations to allow 2-dimensional focussing of a range of x-ray energies to the experimental end stations. By having such a device as close as possible to the source, the largest possible numerical aperture is captured and the flux at the sample for beam sizes of the order of the source size (50-200 $\mu$ m) is dramatically increased. This device can be used in conjunction with a double Laue monochromator to make a high quality beam or with a pinhole to make a broad bandwidth pink beam.

### Side-bounce monochromator

The side-bounce monochromator will take a fixed energy beam into the experimental side-hutch. For the short and extended proposed layouts, the take-off angle of the side-bounce monochromator is 10°, and 5°, respectively. Figure 8 shows the available energies for some silicon monochromator reflections. It can be seen that the advantage of the extended layout, in terms of available beam energies in the side hutch, is quite dramatic. ID15 (ESRF) operates two side-bounce

monochromators with multiple fixed energies using both bent Bragg and Laue crystals; these monochromators also allow the transmission of the white beam to the main hutch. Figure 9 shows the setup used for ID15C. Here, 4 Laue crystals are able to be moved into the beam by vertical translation, giving beam energies in the range of 30-120 keV. Water cooling and crystal benders are incorporated into this tower.

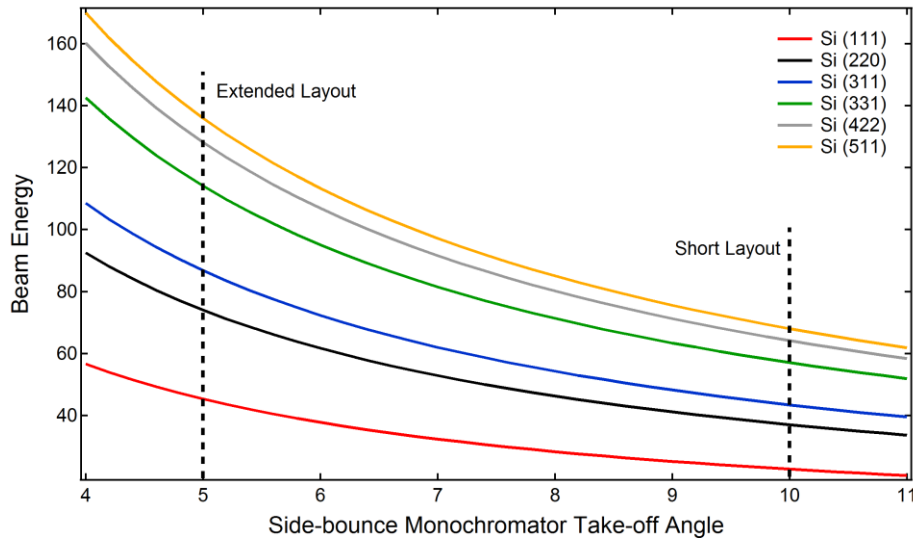


Figure 8. Available energies of various Si crystal reflections. The two proposed take-off angles are shown by vertical dashed lines.

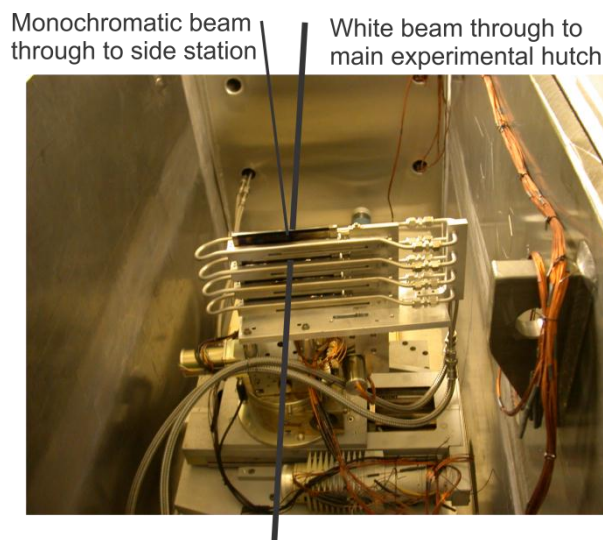


Figure 9. Side bounce monochromator stack operating at ID15C of the ESRF. The white beam travels from the bottom to top of the Figure. Four Laue crystals are vertically offset to allow a range of beam energies into the side station by adjusting the crystal type and reflection.

### Monochromator tank 1

Monochromator tank 1 will house a fixed exit focusing double Laue monochromator system. The double Laue system within the tank should allow both horizontal and vertical offset of the focussed monochromatic beam to give the possibility of; 1) a 1D or 2D focussing system described by Zhong [10, 11] (vertical offset required), which takes advantage of anticlastic bending geometries or 2) a conventional 1D focussing system (preferably horizontal offset).

Mono tank 1 and mono tank 2 will need significant cooling on the primary crystals which are exposed to the white x-ray beam. Most commonly, Laue type monochromators for high-energy x-rays are cooled using gravity fed water to minimise vibrational motion. The ADS should also explore the possibility of cryogenic cooling of the monochromators as demonstrated at I12 of the Diamond Light Source. The advantages of having the crystals at cryogenic temperatures, where a minimum in the coefficient of thermal expansion of silicon exists, needs to be weighed against the operational difficulties the system presents, such as increased risk of failure and vibration.

### **Mirror tank**

A 1D or 2D focussing mirror system should be considered. While this is a technical challenge due to the very small critical angles at energies approaching 150 keV, the potential gain in flux at the sample for energy-dispersive diffraction and white-beam Laue diffraction techniques are potentially 2-3 orders of magnitude. This is based on the assumption of focusing a  $1 \times 1 \text{ mm}^2$  beam at approximately 25 m from the source to a  $0.1 \times 0.1 \text{ mm}^2$  beam on the sample stage at approximately 35 meters from the source. This would provide a polychromatic flux at the sample significantly higher than that available at both ID15 of the ESRF and I12 of Diamond, which do not allow for white beam focussing. The technical challenge of this component will be to extend its reflectivity to energies as high as possible. There will inevitably be a high energy cut-off where the mirror angle is above the critical angle, this will be correlated with the acceptance aperture of the system. Primary calculations for this device should concentrate on this weighting of upper energy limit and acceptance aperture.

### **Monochromator tank 2**

This monochromator will be a bent horizontal fixed-exit double Laue system which takes a focussed beam directly from the transfocator, bypassing the first monochromator tank. The crystals can be bent to Rowland geometry and the crystal thicknesses and asymmetric cuts optimised for a given bandwidth. We would suggest this bandwidth be of the order of 100-300 eV at 100 keV, as most experimental techniques will be resolution limited due to other mechanisms, thus an exceedingly narrow bandwidth below this value is simply flux limiting.

### **Secondary slits**

The secondary slits require the same specifications as the primary slits. The possibility of white beam focussing devices means the powder density at this point in the beam may be similar to that observed by the primary slits.

Secondary slits will also be required for the side station, however, at this point the beam must be monochromatic, thus no heat load issues exist.

### **Experimental hutches**

Schematic layouts of the proposed experimental hutches are shown in Figure 10.

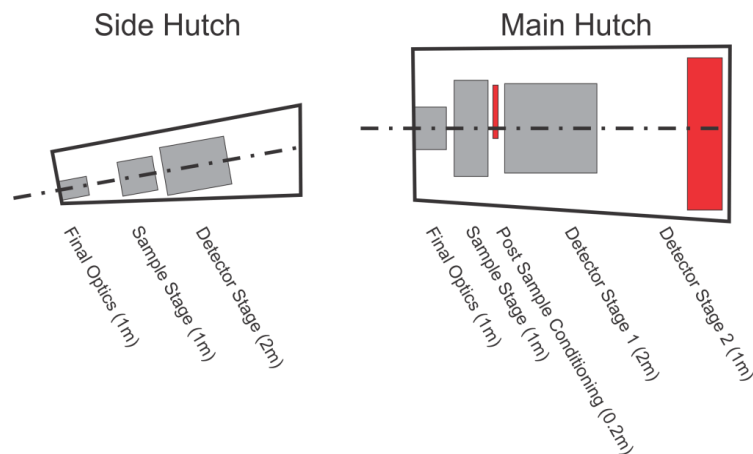


**Figure 10. Schematic layout of experimental hutches. Grey components will always be in use, red components are for optional experiments.**

### **Main hutch**

The main hutch will be the more flexible of the two hutches, and provide access to all the experimental capabilities available at the beamline. This hutch will house;

- 1) An optics table, for any final beam conditioning/monitoring that may be required, e.g. cleaning slits, beam current monitor, short-focus lenses, etc. It is critical that this stage be highly stable with the minimum of vibration.
- 2) A sample stage which is capable of lifting loads of up to 300 kg with a high precision option for accurate positioning and rotation.
- 3) Post sample conditioning optics area for the mounting of slits for energy dispersive diffraction, or analyser crystals, etc.
- 4) A main detector table that holds the detectors for monochromatic and polychromatic diffraction, and for imaging and tomography.
- 5) A secondary detector table that would allow for large horizontal/vertical translation of the monochromatic diffraction detector will also be required at the back of the hutch.

The field of high-energy x-ray scattering techniques is developing fast, thus, the hutch will also contain a large floor space available between the two detector stages for future instrument development and alternative sample environment setups.

### **Side hutch**

The side hutch will be configured to enable monochromatic diffraction experiments, with a focus on multi-dimensional reciprocal space mapping and total scattering analysis. This hutch will house an optics table for any final beam conditioning/monitoring that may be required, a sample stage, and a detector table that holds and translates the detector accurately for monochromatic diffraction. It is envisioned that this hutch will only be used to investigate samples and sample environments of up to 100 kg.

It should also be noted that the shielding requirements for the side hutch are significantly reduced in comparison to the main hutch as only a monochromatic beam, which is a small fraction of the wiggler white beam is capable of being deflected inside.

### **Sample environments**

In order to maximise the utility of the ADS beamline, considerable effort should be made to ensure that a wide range of sample environments are available to users. The experimental hutches will be designed to allow for flexible user setups and easy change over between experiments. The ability to

transfer sample environments between the side and main hutches will greatly enhance the impact of the available facilities. All sample environments should be fully integrated into the beamline control software to allow for universal interfaces and software to be used.

The minimum facilities that should be available are:

- 1) Cryogenic and furnace equipment to cover the temperature range from 10 K to 2000K
- 2) Magnetic field chamber capable of both parallel and perpendicular fields with respect to the beam direction
  - Basic 1 Tesla units are in use at ESRF and other synchrotrons
- 3) Electric field chamber with high-voltage capabilities
- 4) High pressure diamond anvil cell with low- and high-temperature capabilities

As mentioned earlier, one of the major advantages of performing powder diffraction (both monochromatic and energy dispersive) experiments at high x-ray energies is the ability to isolate diffraction information which is recorded at a range of scattering vector orientations to an applied vector field (see Figure 3). This opens up the possibility of rapid detailed anisotropic structural analysis of processes in-situ. Thermo-mechanical deformation is a principle example where the use of high-energy x-rays allows for significant gains in the understanding of the atomic and microstructural processes occurring. We propose that significant funds be allocated to thermo-mechanical testing instruments, including,

- 1) Thermo-mechanical testing instrument (Gleeble)
- 2) High-speed dynamic loading instrument (Bose or Instron)

Availability of sophisticated thermo-mechanical processing equipment as suggested above would set the ADS beamline apart from other high-energy sources and attract international users to the facility as well as develop industrial demand.

The sample environments that are made available at the beamline should be expanded over time as required and supported by the user community. Where possible, sample environments should be constructed to enable operation on other beamlines, such as PD, SAXS/WAXS and IMBL. As a main focus of this beamline will be for *in situ* studies, the handling of toxic, reactive, flammable and/or explosive materials should be anticipated and the ability to vent or flush (small) quantities of gasses should be built into the sample handling of the hutch.

## Detectors

Detection of high-energy x-rays is a significant technical challenge. As energy increases the absorption within the detector materials decreases. At 100 keV, a 1 mm thick silicon based detector will absorb less than 1% of the incident radiation. The most common detection technique, particularly for large area detectors, is to use high density scintillation materials optically coupled to silicon based technologies such as CCD's or CMOS chips.

### Large area high quality

A large area high dynamic range detector is required for the majority of the monochromatic diffraction techniques. The Pixium 4600 from Thales [12] is primarily produced for medical imaging applications in the medium to high energy range. Due to this, it contains a relatively high-Z scintillation material and is approximately 30% efficient at 100 keV. This detector is in use at beamline I12 of the Diamond light source, with an earlier model in use at ID15 of the ESRF [13]. Many other manufacturers produce similar technologies. The major drawback of this detector technology, however, is that its dynamic range is limited to approximately 14bit. Similar technology from Perkin-Elmer [14] is implemented at beamline 11-ID-C of the APS. This company offers

customisation of the detectors for specific purposes and thus can be optimised for high-energy measurements. The downside of this detector is the large pixel size of 200  $\mu\text{m}$  when compared to 140  $\mu\text{m}$  for the Pixium models.

An ADSC Quantum 315 [15] detector may be another possible option (or addition) which could set the ADS beamline apart from other high-energy sources. With scintillators optimised for high x-ray energies, this detector would provide a larger dynamic range, lower noise, and significantly increased spatial resolution over the Pixium 4600 or Perkin-Elmer devices. The frequency of data acquisition is limited to approximately 1 Hz (whereas the above mentioned systems are capable of approx. 10 Hz) however, since we propose to also purchase an ultra-fast acquisition detector the ADSC area detector may make for a better complementary set.

### Large area rapid acquisition

With the advent of CMOS area detectors, there is now the possibility of performing rapid time resolved diffraction experiments using large area detectors. The PCO Dimax camera [16] is capable of 1279 frames/second in full 2016 x 2016 resolution. At smaller RIO's and binning modes the camera is capable of over 150,000 frames/s. It should also be noted that this is the current state of the art, however, the CMOS chip technology has been developing at a high rate over the past 5 years and it would be expected that at the time of purchase the available camera would have superior specifications. By coupling such cameras with suitably fast x-ray to visible light converters, rapid single shot time resolved diffraction utilizing the benefits of monochromatic high-energy x-rays will be possible. At present, the two coupling mechanisms include fast decay image intensifier (currently the prototype system of ID15, ESRF) or scintillator screen with taper optic system. Both of these require some lens coupling to the CMOS camera and developmental costs for this coupling should be included in the projected cost of the detector system. The PCO camera is provided with a software development kit for integration into beamline controls. The BSG are not aware of any integration of this camera into EPICS at other sources.

It should be noted that acquisition at such high frame rates generally means experiments are flux limited. Thus, the maximum possible flux of the source should be a primary goal of both the source and front-end optics choices.

### Multi-element energy resolving

For polychromatic scattering, energy resolving detectors are used to collect scattering information in energy, rather than  $2\theta$  space. A schematic of a typical energy dispersive diffraction setup is shown in Figure 4. Current detector technology for energy dispersive diffraction is highly inefficient in its collection of available scattering information. Therefore, the possibility exists for a dramatic improvement in the quality and speed of data acquisition using this technique. The most advanced detector available for this type of scattering was purchased from Oxford Instruments and is in use at beamline I12 of the Diamond Light Source. This detector is a 23 element germanium energy resolving detector covering an arc of  $180^\circ$  at a fixed diffraction angle of  $5^\circ 2\theta$  to take advantage of the scattering vector orientation dependence described earlier. We propose to purchase a similar systems for the ADS beamline, however, it is possible that with close collaboration with a detector development group a significant increases in the magnitude of solid angle utilised could be gained.

### Imaging

Imaging detectors at high x-ray energies are generally a combination of a scintillation screen and optical imaging system. There is a technical challenge in balancing scintillation efficiency and achievable spatial resolution. Thin scintillators offer high spatial resolution but low efficiency, conversely thick scintillators offer high efficiency but low spatial resolution. The common solution to this is to have a set of scintillation and optics components allowing the switching of the camera for the most suitable experimental setup. The PCO camera, proposed above for rapid diffraction

experiments, will also be ideal for all imaging applications at the ADS beamline, offering rapid imaging capabilities.

### **Beamline control systems**

The ADS beamline will use EPICS as the main control system and employ standardised motion control and communication protocols and solutions as defined by the Australian Synchrotron where appropriate. All efforts will be made to incorporate as many of the sample stages, temperature ancillaries, and detectors into the beamline control systems where EPICS drivers are available. It is estimated that approximately 100 motorised axes will be required to manipulate optics, sample stages and other equipment. Most of the control systems hardware can be purchased 'off the shelf'.

### **Beamline control cabins**

A separate beamline control cabin will be required for the main beamline and also for the side station. Cabins are required for user comfort and house Operator Interfaces (OPIs) used to control the optics, sample stages and other beamline systems.

### **Commercial data analysis software and licenses**

Several useful commercial software packages are desirable to assist user experiments. Some of these require continual license renewal, while others can be purchased outright. Required packages include:

- International Centre for Diffraction Data (ICDD) database access coupled with a search/match package such as HighScore from Panalytical for powder diffraction pattern phase identification.
- Inorganic Crystal Structure database (ICSD)
- Cambridge Structural database (CSD)
- Total Pattern Analysis (TOPAS) from Bruker AXS for structural refinement and structure solution.

### **Laboratory infrastructure**

#### **Solid sample preparation**

It is expected that the majority of the experimental work carried out at the beamline will be on bulk materials, both metals and ceramics. Thus, basic sample preparation equipment for these types of materials should be included. Suggested equipment,

- 1) Precision diamond saw
- 2) Basic grinding and polishing equipment
- 3) Large working distance optical microscope
- 4) Spot welder for thermocouples

#### **Chemistry**

Basic wet chemistry laboratory space would also be required, particularly for total scattering experiments on liquids where samples often have to be prepared a very short time prior to experimentation.

#### **Experimental preparation**

One of the major proposed ancillary components of the beamline is the thermo-mechanical deformation and testing instrument. This is a complex instrument and should have its own "off beam" laboratory for preliminary data collection and training of users prior to the beginning of their beamtime. Depending on the type of instrument purchased, this space may vary in size from 6 to 10

square meters. The laboratory housing this instrument should also have the capabilities of water cooling, gas systems, and ventilation.

### Data transfer requirements

Large area monochromatic and multi-element energy dispersive detectors produce a large amount of data in a relatively short period of time. As an example, the proposed high-speed area detector proposed above is capable of producing over 1000 frames/s at a resolution of 2016 x 2016 pixels. Assuming 16 bit image resolution, this equates to a peak data acquisition rate in excess of 60 GBit/s.

Dedicated 10 GBit links between the beamline detector PC's and the main data servers would be necessary. This will also enable users to make immediate use of the large-scale computing facilities offered by the Australian Synchrotron for data reduction and preliminary analysis.

### Preliminary costings

The following cost estimates for critical components have been collated. These numbers have come from the Australian Synchrotron based on the costs of the IMBL, and through private communication with beamline staff at the ESRF and Diamond Light Sources.

| <b>Component</b>  | <b>Facility</b> | <b>Currency</b> | <b>Cost<br/>(,000's)</b> | <b>Cost (,000's<br/>AUD)</b> |
|---|-----------------|-----------------|--------------------------|------------------------------|
| <b>Superconducting Wiggler (Budka)</b>  | AS              | AUD             | 1300                     | 1300                         |
| <b>Front end apertures (mask), ion pump, BPMs and diamond window</b>  | AS              | AUD             | 180                      | 180                          |
| <b>Shielding (Caratelli)</b>  | AS              | AUD             | 1100                     | 1100                         |
| <b>Vacuum systems (Varian)</b>  | AS              | AUD             | 180                      | 180                          |
| <b>Beamline control systems (Delta Tau)</b>   | AS              | AUD             | 500                      | 500                          |
| <b>Fitted out control cabins (x 2)</b>  | AS              | AUD             | 250                      | 250                          |
| <b>Low energy absorber</b>  | ESRF/JEEP       | EUR             | 150                      | 205.5                        |
| <b>Transfocator tank and compound lenses</b>  | ESRF            | EUR             | 200                      | 274                          |
| <b>Cryo-mono tanks, crystals and cooling system</b>   | JEEP            | GBP             | 500                      | 785                          |
| <b>Mirror tank and mirrors (estimate, as may require development)</b>   | AS              | AUD             | 250                      | 250                          |
| <b>Side hutch mono tank and crystal stack</b>   | Estimated       | AUD             | 300                      | 300                          |
| <b>Slits and shutters</b>   | JEEP            | EUR             | 150                      | 205.5                        |
| <b>Beam diagnostics (current and position monitors)</b>   | Estimated       | AUD             | 300                      | 300                          |
| <b>Huber precision sample stack</b>   | JEEP            | EUR             | 140                      | 191.8                        |
| <b>Heavy lift sample stage (lower precision)</b>  | JEEP            | EUR             | 150                      | 205.5                        |
| <b>Large detector stage set</b>   | JEEP            | USD             | 300                      | 288                          |
| <b>Side hutch optics, sample, and detector stages (estimate)</b>  | Estimated       | AUD             | 250                      | 250                          |
| <b>Large area detector for monochromatic diffraction (Pixium from Thales or similar) x 3 for main and side stations</b> | JEEP            | EUR             | 450                      | 616.5                        |

|   |           |     |              |              |
|---|-----------|-----|--------------|--------------|
| <b>PCO Dimax for ultra-fast diffraction and imaging</b>   | ESRF      | EUR | 80           | 109.6        |
| <b>Scintillation coupling systems for ultra-fast diffraction and imaging</b>                      | ESRF/JEEP | EUR | 150          | 205.5        |
| <b>23 element energy dispersive detector (suggest collaborative development alternative)</b>      | JEEP      | GBP | 220          | 345.4        |
| <b>23 channel XIA electronics for ED detector (suggest collaborative development alternative)</b> | JEEP      | GBP | 80           | 125.6        |
| <b>Slit system for polychromatic energy dispersive scattering</b>                                 | JEEP      | GBP | 30           | 47.1         |
| <b>Cryostats, pressure, magnetic and electric field cells</b>                                     | Estimated | AUD | 300          | 300          |
| <b>Thermo mechanical testing instrument</b>   | Estimated | AUD | 1000         | 1000         |
| <b>Dynamic mechanical testing instruments (Bose 3kN)</b>  | UNSW      | AUD | 200          | 200          |
| <b>Laboratory equipment</b>   | Estimated | AUD | 300          | 300          |
| <b>Software packages</b>  | Estimated | AUD | 20           | 20           |
|   |           |     | <b>Total</b> | <b>10035</b> |

## Non-critical components

There would be several options to reduce the initial cost of the beamline and allow for future expansion to the complete suite of operations. These are listed below in order of preference of elimination,

- 1) Fitting out and operation of monochromatic side station, we highly recommend the shielding be in place for future expansion however. All experiments possible in the side station are also possible in the main hutch. This also removes the need for one area detector.
- 2) White beam focussing device. Many of the polychromatic experiments can still be performed in the slitted down white beam.
- 3) Energy dispersive diffraction setup. Since the majority of the scattering work done at the highlighted similar beamlines are in monochromatic mode, all energy dispersive capabilities could be built later. This, however, will significantly limit the attraction for industrial research.

## Conceptual design

The above report outlines the proposed critical components of the ADS beamline. Preliminary engineering resources need to be allocated to the following components,

- 1) Quantification of performance enhancements achieved by extending the beamline beyond the footprint available within the experimental hall
- 2) Front end design and heat-load management

- 3) Low energy absorber and filters
  - a. Optimization of flux profiles for various arrangements
  - b. Finite element analysis of heat load on optimum absorbers
  - c. Assessment of whether these components could go in the front end. Would be helpful to save space where possible in the optics hutch.
- 4) Transfocator lens design, i.e. number and type of lenses to give a versatile range of focal energies
- 5) Monochromators
  - a. Finite element analysis of heat loads on proposed monochromators and the resulting distortions to the crystals
    - i. Side hutch monochromators
    - ii. Mono Tank 1 focusing double Laue monochromators
    - iii. Mono Tank 2 Rowland double Laue monochromators
  - b. Optimization of crystal cuts and bending geometries given these distortions
  - c. All above calculations performed for water and cryo cooling to decide on optimum system for the given source
  - d. Analysis of the effect of vibration from the cooling system on the beam quality
- 6) Calculation of possible mirror geometries to gain flux in typical polychromatic beam sizes of 10-100 $\mu$ m at the sample position. Primary calculations for this device should concentrate on this weighting of upper energy limit and acceptance aperture.
  - a. Heat load requirements/distortions
- 7) Hutch radiation shielding calculations (should be similar to IMBL depending on their front end aperture of that beamline)

The BSG has some expertise in performing the above calculations. John Daniels has significant experience in basic calculations for absorbers, lenses, monochromators, and heat load modelling. Item 5 of the above conceptual design requirements is by far the most critical and complicated. These calculations should be cross checked with beamline scientists with previous knowledge in design and application of such monochromators. People with previous knowledge in the area and collaborate with those in the BSG include Veijo Honkimäki (ESRF), Marci DiMichiel (ESRF), Michael Drakopolous (Diamond). Other facilities which may have suitable people for these calculations are included in the beamline list below.

## Similar beamlines

An initial survey of existing and planned beamlines with similar scope and capabilities to the Advanced Diffraction and Scattering (ADS) beamline has been completed. Eight representative beamlines were chosen. These were selected primarily on the basis of the planned scientific programme and the accessible energy range of the beamlines. There was also consideration given for the comparative capability of the host facility: the storage ring energy and beam current. The eight beamlines (listed in Table 1) are comprised of seven international facilities and the Imaging and Medical beamline (IMBL) at the Australian Synchrotron. Although the scientific scope of IMBL is significantly different compared to the ADS beamline, there are many similarities, especially at the front end with respect to the source, energy range, shielding and the heat load reduction strategy. This information will be particularly useful in the design phase of the project.

| <u>Beamline</u>   | <u>Facility</u>           |
|---|---------------------------|
| <b>Joint Engineering, Environmental and Processing (JEEP)</b> | I12, Diamond light Source |
| <b>Imaging and Medical (IMBL)</b>                             | Australian Synchrotron    |
| <b>Extreme Conditions</b>                                     | I15, Diamond light Source |

|  |                       |
|--|-----------------------|
| <b>High Energy Materials Science (HEMS)</b>                  | P07, Petra III        |
| <b>High Energy and Diffraction and Scattering (HEDS) - A</b> | ID15A, ESRF           |
| <b>High Energy and Diffraction and Scattering (HEDS) - B</b> | ID15B, ESRF           |
| <b>BESSC-CAT, PDF Beamline</b>                               | ID-11-B, APS          |
| <b>X-ray Powder Diffraction (XPD)</b>                        | NSLS II               |
| <b>X-ray Powder Diffraction side station (XPD-ss)</b>        | NSLS II, side station |

We believe that the proposed experimental layouts of the beamline given within this document will allow Australian users access to a high-energy x-ray source which will meet or exceed the capabilities of the above mentioned beamlines in several areas. We also believe, that by providing unique detector and sample environment capabilities, that the ADS beamline will attract international users whom don't have access to these facilities within their own countries.

## Example studies

Several of the example studies presented below were performed at overseas high-energy x-ray sources by Australian user groups, and highlight the unique features of the proposed source as a tool for materials analysis. Additional studies are presented from international users to show the breadth of possible experimentation that the ADS beamline will support. The beamline will open fields of research previously untapped or underutilised in Australia and will maintain Australia's place at the forefront of diffraction-based research.

## Total scattering analysis

### Negative thermal expansion materials - Kepert, University of Sydney

Negative thermal expansion (NTE) is an exotic material property with attractive potential applications, most notably in moderating the predominantly positive thermal expansion of materials, particularly those in high precision applications where instability associated with temperature fluctuation often reduces performance. This behaviour has been identified in a range of oxide-based materials, as well as molecular framework materials containing linear diatomic bridges such as the cyanide anion.

An *In situ* total scattering study of  $\text{Zn}(\text{CN})_2$  was carried out in order to identify the mechanism by which the NTE was exhibited. It was found that the C/N that bridge between the Zn centres showed an increase in average transverse displacement with increasing temperature (Figure 11) giving direct confirmation of this mechanism for NTE[17] - structural information extracted directly from the PDFs. The rich structural and compositional diversity of cyanide-bridged molecular framework materials is expected to yield a vastly expanded range of NTE materials with enhanced properties and, as such, the study of the mechanism underlying the NTE in the cyanide-bridged  $\text{Zn}(\text{CN})_2$  structure is of particular relevance.

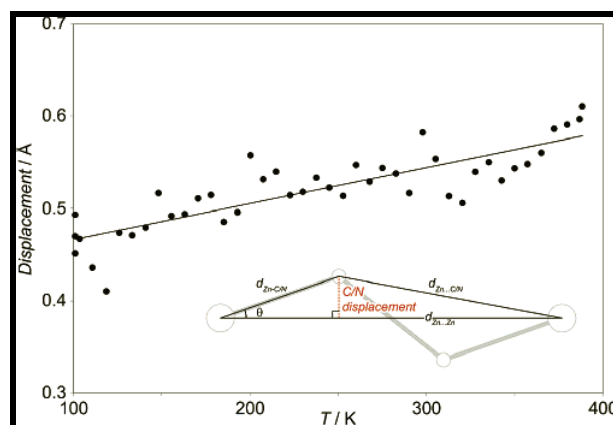


Figure 11: Average displacement of the C/N bridging atoms from the line connecting the ZnII centres.

This work was enabled by access to high energy X-rays which allowed the total scattering analyses. The ADS beamline would give access to the X-rays required to carry out this experiment.

Chapman, K. W., Chupas, P. J. & Kepert, C. J. 2005, 'Direct Observation of a Transverse Vibrational Mechanism for Negative Thermal Expansion in  $\text{Zn}(\text{CN})_2$ : An Atomic Pair Distribution Function Analysis', *Journal of the American Chemical Society*, vol. 127, pp. 15630-15636.

### Atomic anisotropy of thermal expansion in bulk metallic glass –Liss, ANSTO

Glass transition temperature and plastic yield strength are known to be correlated in metallic glasses. We have observed by in-situ synchrotron high energy X-ray diffraction and pair distribution analysis anisotropy of the thermal expansion behavior in the nearest neighbor and second nearest neighbor atomic distances in the building blocks of Zr-Cu-Ni-Al based bulk metallic glass, leading inevitably to shear. Mechanical yielding of the latter on the atomic scale leads to the glass transition and the increase of the free volume. These experimental results uncover the mechanism, how glass transition and yield strength are linked.

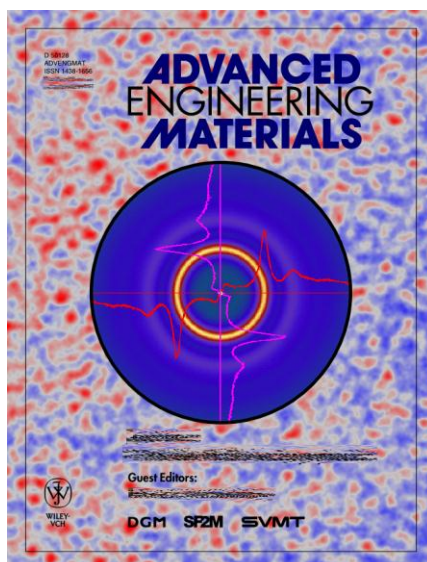


Figure 12. The background image confirms the irregular amorphous structure of a bulk metallic glass in a false-color transmission electron micrograph (scale: 10 nanometer horizontally across the page). Atomic rearrangements at the glass transition were studied in real time by in-situ high energy X-ray diffraction. A two-dimensional pattern showing the typical broad rings scattered by the amorphous material is represented in the center, from which average atomic distances can be concluded accurately

Dongdong Qu, Klaus-Dieter Liss, Kun Yan, Mark Reid, Jonathan D. Almer, Yanbo Wang, Xiaozhou Liao, Jun Shen: "On the atomic anisotropy of thermal expansion in bulk metallic glass", *Advanced Engineering Materials* (2011)

## Single crystal diffuse scattering

### Relaxor ferroelectrics and other functional oxide ceramics - Welberry, ANU

A renewed interest in the field of ferroelectricity has taken place in recent years since the finding of exceptional piezoelectric properties in the lead-oxide class of relaxor ferroelectric (RF) materials typified by the disordered perovskites  $\text{PbMg}_{1/3}\text{Nb}_{2/3}\text{O}_3$  (PMN) and  $\text{PbZn}_{1/3}\text{Nb}_{2/3}\text{O}_3$  (PZN). RFs are materials having an extremely high dielectric constant that has significant dispersion over a broad range of frequency and exists over a wide range of temperature. When doped with  $\text{PbTiO}_3$  (a conventional ferroelectric material), PMN and PZN can exhibit high strain levels, making them promising candidates for the next generation of solid-state transducers and actuators. Although PMN, PZN and numerous related materials have been extensively studied over a long period, a detailed understanding of the exact nature of their polar nanostructure has still not emerged.

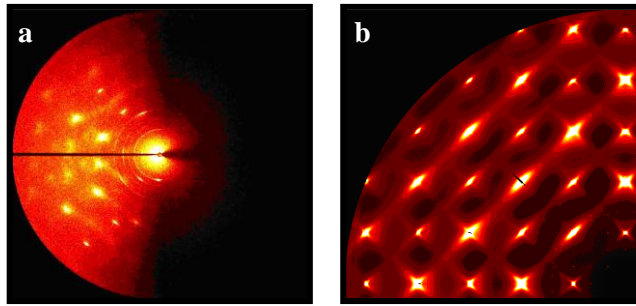


Figure 13: (a) A single frame of data for PZN-PT using 25 keV X-rays. (b) Part of a full 3-dimensional data set of PZN recorded using 58 keV X-rays. The relative intensity scales are 1:150

All of the important materials of this kind are based on Lead, or more recently, on Bismuth. Both Pb and Bi are strong absorbers of low-energy (< 25 keV) X-rays, so in order to obtain good diffuse scattering data, much higher-energy X-rays must be used. Figure 13(a) shows data collected at 25 keV at the AS PD beamline; most of the field of view is blocked by the shadow of the crystal, the signal level is very low and there is strong powder scattering from surface damage on the outside of the cut crystal. In contrast, Figure 13(b) is of a comparable sized sample of PZN recorded at the APS using 58 keV X-rays. Access to the higher energies and intensities at the ADS beamline allow the diffuse scattering signal to be recorded with excellent signal to noise and shows much fine-detail that is crucial to the analysis.

Pasciak, M. & Welberry, T. R. 2011, 'Diffuse scattering and local structure modelling in ferroelectrics', *Zeitschrift für Kristallographie*, vol. 226, pp. 113-125.

## Materials mapping and texture analysis

### Study of residual strain in thermal barrier coatings - Thornton, DSTO

Thermal barrier coatings (TBCs) typically consist of a 0.3 mm layer of partially stabilised zirconia over a bond coat of 0.2 mm of NiCoCrAlY applied to a metal substrate. TBCs are applied to components that are exposed to hot combustion gases within gas turbine and piston engines in order to thermally insulate the components. While TBCs are now widely used, their lifetime cannot be predicted reliably. The ability to predict TBC lifetimes will enable a greater utilisation of the coating's temperature reduction properties and requires a full understanding of the failure mechanisms of TBCs.

Studies of the residual strains in the zirconia layer, carried out low energies, were limited to the top 50  $\mu\text{m}$ . Neutron measurements were conducted on 1 mm thick layers, and did show a strain gradient through the layer. In order to map the phase composition, and obtain information on the magnitude and distribution of the strains, high energy X-rays (*ca.* 80 keV) were used in transmission geometry to provide sufficient penetration.

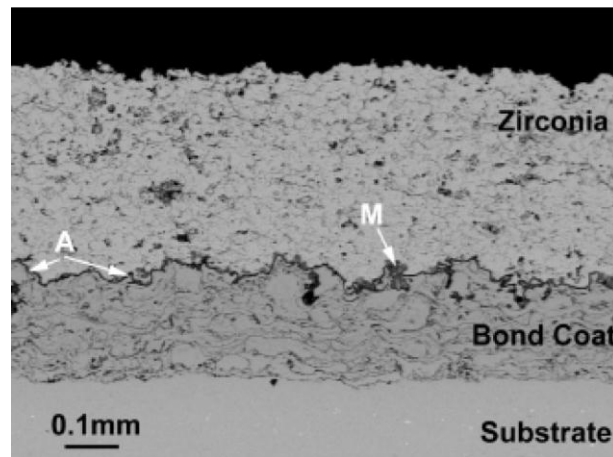


Figure 14: A cross-section of the heat-treated sample showing a thin band of alumina (A) covering the bond coat.

This experiment observed out-of plane tensile strains at, and above, the interface, supporting the proposed mechanisms for TBC failure based on localised swelling of the material underlying the zirconia.

To continue this work requires access to high energy x-rays, as would be available at the ADS beamline, in order to penetrate the thick samples. Reflection-geometry methods using lower energy X-rays are not feasible due to the limited volume sampled by that mode. Additionally, energy-dispersive diffraction will further aid localisation of the strains though the gauge volume formed in this geometry.

Thornton, J., Slater, S. & Almer, J. 2005, 'The Measurement of Residual Strains within Thermal Barrier Coatings Using High-Energy X-Ray Diffraction', *Journal of the American Ceramic Society*, vol. 88, no. 10, pp. 2817-2825.

### Phase transitions in metal alloys - Liss, ANSTO

Low density, high specific yield strength, high oxidation resistance, and good creep properties at elevated temperatures make intermetallic  $\gamma$ -TiAl-based alloys excellent candidates as structural materials for advanced jet and automotive engines as well as for future hypersonic vehicles. The mechanical properties depend strongly on composition, thermo-mechanical processing, and subsequent heat treatment. The processes occurring during heat treatment are complex and difficult to study directly. Therefore, characterisation and measurements are necessary with different techniques such as macroscopic stress and strain measurements, hardness testing, optical and electron microscopy, calorimetry, as well as diffraction methods with neutrons and X-rays, to mention but a few.

High-energy X-rays (> 100 keV) can penetrate centimetres into light and medium-dense materials as investigated here. The high flux and intensity of modern sources give rise to high spatial and angular resolutions at high acquisition rates. The combination of the penetration power into a bulk sample and the large number of photons available allow for sophisticated, novel *in situ* investigations, as was performed in this study on a massively transformed  $\gamma$ -TiAl based alloy.



Figure 15: Diffraction ring triplet showing correlations between the  $\gamma$  - and  $\alpha$ -phases.

A high-energy synchrotron X-ray diffraction study was undertaken at ID15B at the ESRF to characterise *in situ* phase transitions, recrystallisation behaviour, and phase evolution in an intermetallic Ti–46Al–9Nb alloy up to 1400 °C. This work has revealed the rich phase transformation and recrystallisation behaviour of these materials. The diffraction information shows coherences between different phases and domains in the material, which are attributed to internal stresses and chemical imbalances.

This work is only possible through the use of high-energy (ca. 90 keV) X-rays and *in situ* furnaces and applied-load instrumentation.

Liss, K.-D., Bartels, A., Clemens, H., Bystrzanowski, S., Stark, A., Buslaps, T., Schimansky, F.-P., Gerling, R., Scheu, C. & Schreyer, A. 2006, 'Recrystallization and Phase Transitions in a  $\gamma$ -TiAl-Based Alloy as Observed by Ex Situ and in Situ High-Energy X-Ray Diffraction', *Acta Materialia*, vol. 54, pp. 3721-3735.

### 2D mapping of strain distributions in Zr-hydrides – Daniels, UNSW

The strains in matrix and hydrides around a fatigue crack tip grown *in-situ* in a single-edge notched specimen of hydrided Zircaloy-4 were determined using high-energy synchrotron x-ray diffraction at various stages of loading. The hydride phase shows proportionally larger strains at full load compared to the matrix strain. The residual strains of the matrix ahead of the crack tip reveal the reverse plastic zone for a crack grown in tension, while the hydride residual strains remain strongly tensile.

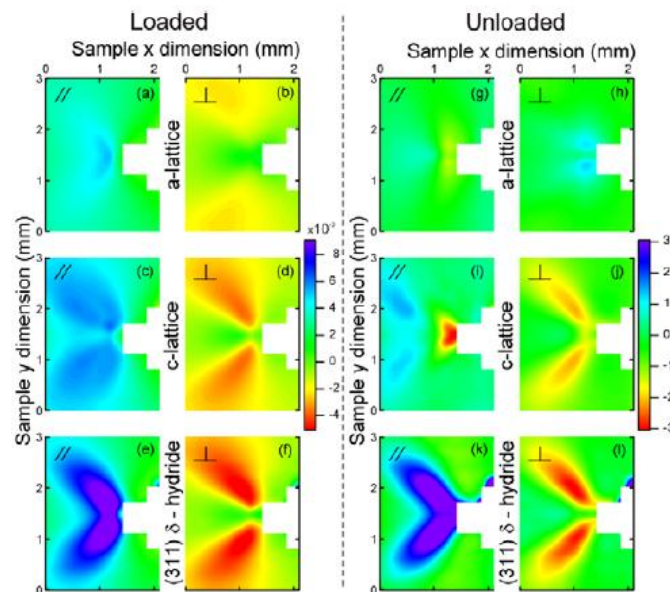


Figure 16. A map of the lattice strain in the longitudinal (crackopening) and transverse direction strain at the crack tip under load (left) and after unloading (right) for the matrix lattice parameters a, c (top, middle) and hydride d-311 lattice spacing (bottom).

A. Steuwer, J. E. Daniels, M. J. Peel, "In-situ crack growth studies of hydrided Zircaloy-4 on a single-edge notched tensile specimen", *Scripta Materialia*, **61-4**, 431-433 (2009)

## Energy dispersive diffraction

### Passivation layers in inert anodes - Rowles, CSIRO

Traditionally, most characterisation of starting materials and products for electrochemical investigations in molten salts relies upon *ex-situ* techniques. Information obtained in this manner is

often subject to experimental artefacts brought about by changes that may take place during preparation of samples for analysis. Whilst *in situ* techniques are common in aqueous electrochemistry, equivalent methods for molten-salt electrochemistry are particularly challenging due to the high temperatures and corrosive materials.

In this work, a high energy, energy-dispersive diffraction experiment was undertaken at I12, JEEP at the Diamond Light Source, in order to study the transformation of Magnéli-phase anodes ( $\text{Ti}_n\text{O}_{2n-1}$ ;  $n=4-6$ ) in an operational titanium electrowinning cell in molten  $\text{CaCl}_2$  at 950 °C. This work takes advantage of the isolated gauge volume, measuring diffraction information only from the anode, whilst ignoring scattering from the furnace and other parts of the cell.

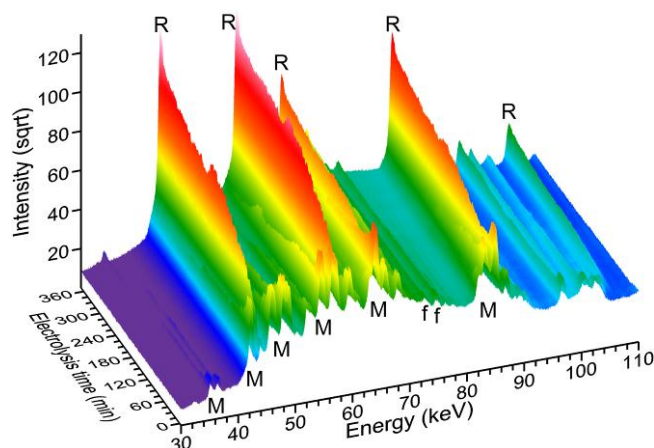


Figure 17. Accumulated patterns collected for a cell collected over 6 hours. The original Magnéli phases can be seen transforming into rutile.

This work observed the growth of a rutile ( $\text{TiO}_2$ ) layer on the anode through the oxidation of the Magnéli phases. Rietveld analysis of the diffraction data revealed the thickness of this layer as a function of time, and allowed a kinetics analysis which showed that the layer growth is limited by oxygen diffusion.

The materials and physical dimensions of the cells used in this experiment demand access to high energy X-rays in order to penetrate the sample cell and electrolyte, typically  $\text{CaCl}_2$ . Additionally, energy dispersive diffraction simplifies the sample cell design as it demands only a single, small beam exit window. Access to a high-energy beamline capable of delivering polychromatic X-rays, with an energy dispersive detector would enable this experiment to be carried out in Australia.

Scarlett, N. V. Y., Madsen, I. C., Evans, J. S. O., Coelho, A. A., McGregor, K., Rowles, M. R., Lanyon, M. R. & Urban, A. J. 2009, 'Energy Dispersive Diffraction Studies of Inert Anodes', *Journal of Applied Crystallography*, vol. 42, pp. 502-512.

Rowles, M. R., Styles, M. J., Madsen, I. C., Scarlett, N. V. Y., McGregor, K., Riley, D. P., Snook, G. A., Urban, A. J., Connolly, T. & Reinhard, C. 2011, 'Quantification of Passivation Layer Growth in Inert Anodes for Molten Salt Electrochemistry by In Situ Energy-Dispersive Diffraction', *Journal of Applied Crystallography*, submitted.

## International studies

### Strain in amorphous materials - Poulsen, Risø National Laboratory

Abstract: A number of properties of amorphous materials including fatigue, fracture and component performance are governed by the magnitude of strain fields around inhomogeneities such as inclusions, voids and cracks. At present, localized strain information is only available from surface

probes such as optical or electron microscopy. This is unfortunate because surface and bulk characteristics in general differ. Hence, to a large extent, the assessment of strain distributions relies on untested models. Here we present a universal diffraction method for characterizing bulk stress and strain fields in amorphous materials and demonstrate its efficacy by work on a material of current interest in materials engineering: a bulk metallic glass. The macroscopic response is shown to be less stiff than the atomic next-neighbour bonds because of structural rearrangements at the scale of 4–10 Å. The method is also applicable to composites comprising an amorphous matrix and crystalline inclusions.

Poulsen, H. F., Wert, J. A., Neuefeind, J., Honkimäki, V. & Daymond, M. 2005, 'Measuring strain distributions in amorphous materials', *Nature Materials*, vol. 4, pp. 33-36.

### **Combined X-ray diffraction and imaging - Ludwig, ESRF**

Abstract: Non-destructive, three-dimensional (3D) characterization of the grain structure in mono-phase polycrystalline materials is an open challenge in material science. Recent advances in synchrotron based X-ray imaging and diffraction techniques offer interesting possibilities for mapping 3D grain shapes and crystallographic orientations for certain categories of polycrystalline materials. Direct visualisation of the three-dimensional grain boundary network or of two-phase (duplex) grain structures by means of absorption and/or phase contrast techniques may be possible, but is restricted to specific material systems. A recent extension of this methodology, termed X-ray diffraction contrast tomography (DCT), combines the principles of X-ray diffraction imaging, three-dimensional X-ray diffraction microscopy (3DXRD) and image reconstruction from projections. DCT provides simultaneous access to 3D grain shape, crystallographic orientation and local attenuation coefficient distribution. The technique applies to the larger range of plastically undeformed, polycrystalline mono-phase materials, provided some conditions on grain size and texture are fulfilled. The straightforward combination with high-resolution microtomography opens interesting new possibilities for the observation of microstructure related damage and deformation mechanisms in these materials.

Ludwig, W., King, A., Reischig, P., Herbig, M., Lauridsen, E. M., Schmidt, S., Proudhone, H., Forest, S., Cloetens, P., Rolland Du Roscoat, S., Buffière, J. Y., Marrow, T. J. & Poulsen, H. F. 2009, 'New Opportunities for 3D Materials Science of Polycrystalline Materials at the Micrometre Lengthscale by Combined Use of X-Ray Diffraction and X-Ray Imaging', *Materials Science and Engineering A*, vol. 524, pp. 69-76.

### **Anomalous diffraction at ultra-high energy for protein crystallography - Jakoncic**

Abstract: Single-wavelength anomalous diffraction (SAD), multiwavelength anomalous diffraction (MAD) and single isomorphous replacement with anomalous scattering (SIRAS) phasing at ultra-high X-ray energy, 55 keV, are used successfully to determine a high-quality and high-resolution experimental electron density map of hen egg-white lysozyme, a model protein. Several combinations, between single- and three-wavelength, with native data were exploited to demonstrate that standard phasing procedures with standard equipment and software can successfully be applied to three-dimensional crystal structure determination of a macromolecule, even at these very short wavelengths. For the first time, a high-quality three-dimensional molecular structure is reported from SAD phasing with ultra-high-energy X-rays. The quality of the crystallographic data and the experimental electron density maps meet current standards. The 2.7% anomalous signal from three Ho atoms, at the Ho *K* edge, was sufficient to obtain a remarkable electron density and build the first lanthanide structure for HEWL in its entirety.

Jakoncic, J., Di Michiel, M., Zhong, Z., Honkimaki, V., Jouanneau, Y. & Stojanoff, V. 2006, 'Anomalous Diffraction at Ultra-High Energy for Protein Crystallography', *Journal of Applied Crystallography*, vol. 39, no. 6, pp. 831-841.

### 3D Grain mapping by toptotomography - Ludwig, ESRF

Abstract: By orienting a crystal grain with its diffraction vector along the sample rotation axis, it is possible to use powerful tomographic and topographic imaging techniques to reconstruct the three-dimensional grain shape inside a polycrystalline sample. The acquisition and reconstruction can be performed from projection images with the detector positioned either in the diffracted-beam or in the direct-beam position. In the first case, the projection data consist of a series of integrated, monochromatic beam X-ray diffraction topographs of the grain under investigation. In the second case, the corresponding diffraction contrast in the transmitted beam may be interpreted as an additional contribution to the X-ray attenuation coefficient of the material. This latter variant is restricted to grains with small orientation spread but offers the possibility to characterize simultaneously the three-dimensional grain shape and the absorption microstructure of the surrounding sample material. The contrast mechanism is sensitive to local strain fields and can, in certain cases, reveal details of the grain microstructure, such as the presence of second-phase inclusions. The methodology is successfully demonstrated on an aluminium polycrystal, with a resulting three-dimensional mapping accuracy better than 7 nm. The possibilities and limitations of the technique are listed and its performance relative to other three-dimensional mapping techniques is discussed.

Ludwig, W., Mejdal, E., Soeren, L., Henning, S., Poulsen, F. & Baruchel, J. 2007, 'High-Resolution Three-Dimensional Mapping of Individual Grains in Polycrystals by Topotomography', *Journal of Applied Crystallography*, vol. 40, pp. 905-911.

### Uniaxial stress at high temperature and pressure - Grima Gallardo, Universidad de Los Andes

Abstract: The uniaxial stress components (USC),  $t$ , have been measured in NaCl samples, under variable pressure and temperature, in tungsten carbide (WC) toroidal anvils by energy dispersive X-ray diffraction under synchrotron radiation in a large volume Paris-Edinburgh cell. It was observed that  $t$  increases with load and at  $p = 4.6$  GPa,  $t = -0.6$  GPa (measured from the mean value of the lattice parameter of NaCl). When heating is applied (under load),  $t$  decreases, and becomes zero for  $T < 600$  K. On cooling at constant load,  $t$  remains negligible ( $t = 0.01$  GPa) down to room temperature. After loading again ( $p = 3.8$  GPa) at room temperature,  $t$  remains small ( $t = -0.07$  GPa). A measurement of the FWHM of the diffraction peaks verifies the improvement in hydrostaticity after heating.

Grima Gallardo, P., Besson, J. M., Itié, J. P., Gauthier, M., Mézouar, M., Klotz, S., Häusermann, D. & Hanfland, M. 2000, 'Uniaxial Stress Component in WC Toroidal Anvils under High Pressure and Temperature', *Physica Status Solidi A*, vol. 180, no. 2, pp. 427-437.

### X-ray diffraction contrast tomography - Ludwig, ESRF & Johnson, University of Manchester

Abstract: The principles of a novel technique for nondestructive and simultaneous mapping of the three-dimensional grain and the absorption microstructure of a material are explained. The technique is termed X-ray diffraction contrast tomography, underlining its similarity to conventional X-ray absorption contrast tomography with which it shares a common experimental setup. The grains are imaged using the occasionally occurring diffraction contribution to the X-ray attenuation coefficient each time a grain fulfils the diffraction condition. The three-dimensional grain shapes are reconstructed from a limited number of projections using an algebraic reconstruction technique. An algorithm based on scanning orientation space and aiming at determining the corresponding crystallographic grain orientations is proposed. The potential and limitations of a first approach, based on the acquisition of the direct beam projection images only, are discussed in this first part of the paper. An extension is presented in the second part of the paper [Johnson, King,

Honnicke, Marrow & Ludwig (2008). *J. Appl. Cryst.* 41, 310–318], addressing the case of combined direct and diffracted beam acquisition.

Ludwig, W., Schmidt, S., Lauridsen, E. M. & Poulsen, H. F. 2008, 'X-Ray Diffraction Contrast Tomography: A Novel Technique for Three-Dimensional Grain Mapping of Polycrystals. I. Direct Beam Case', *Journal of Applied Crystallography*, vol. 41, pp. 302-309.

Abstract: By simultaneous acquisition of the transmitted and the diffracted beams, the applicability of the previously introduced diffraction contrast tomography technique [Ludwig, Schmidt, Lauridsen & Poulsen (2008). *J. Appl. Cryst.* 41, 302–309] can be extended to the case of undeformed polycrystalline samples containing more than 100 grains per cross section. The grains are still imaged using the occasionally occurring diffraction contribution to the X-ray attenuation coefficient, which can be observed as a reduction in the intensity of the transmitted beam when a grain fulfils the diffraction condition. Automating the segmentation of the extinction spot images is possible with the additional diffracted beam information, even in the presence of significant spot overlap. By pairing the corresponding direct ('extinction') and diffracted beam spots a robust sorting and indexing approach has been implemented. The analysis procedure is illustrated on a real data set and the result is validated by comparison with a two-dimensional grain map obtained by electron backscatter diffraction.

Johnson, G., King, A., Honnicke, M. G., Marrow, J. & Ludwig, W. 2008, 'X-Ray Diffraction Contrast Tomography: A Novel Technique for Three-Dimensional Grain Mapping of Polycrystals. II. The Combined Case', *Journal of Applied Crystallography*, vol. 41, pp. 310-318.

## References

1. Honkimaki, V., *Personal Communication*, J. Daniels, Editor. 2011.
2. Honkimaki, V. *UPBL2: High energy beamline for buried interface structures and materials processing*. 2010; Available from: [http://www.esrf.eu/UsersAndScience/Experiments/StructMaterials/beamline-portfolio/CDR\\_UPBL02.pdf](http://www.esrf.eu/UsersAndScience/Experiments/StructMaterials/beamline-portfolio/CDR_UPBL02.pdf).
3. Peele, A., *ISAP statistics*. 2011.
4. Drakopolous, M., *Personal Communication*, J. Daniels, Editor. 2011.
5. Liss, K.-D., et al., *High energy X-rays: A tool for advanced bulk investigations in materials science and physics*. Textures and Microstructures, 2003. **35** p. 219-252.
6. Pyzalla, A., W. Reimers, and K.-D. Liss, *A comparison of neutron and high-energy synchrotron radiation as tools for texture and stress analysis*. Materials Science Forum, 2000. **347**: p. 34-39
7. Scarlett, N.V.Y., et al., *Energy Dispersive Diffraction Studies of Inert Anodes*. Journal of Applied Crystallography, 2009. **42**: p. 502-512.
8. Poulsen, H.F., D.J. Jensen, and G.B.M. Vaughan, *Three-dimensional X-ray diffraction microscopy using high-energy X-rays*. MRS Bulletin, 2004. **29**(3): p. 166-9.
9. Vaughan, G.B.M., et al., *X-ray transfocators: focusing devices based on compound refractive lenses*. Journal of Synchrotron Radiation, 2011. **18**: p. 125-133.
10. Zhong, Z., et al., *Sagittal focusing of high-energy synchrotron X-rays with asymmetric Laue crystals. II. Experimental studies*. Journal of Applied Crystallography, 2001. **34**: p. 646-653.
11. Zhong, Z., et al., *Sagittal focusing of high-energy synchrotron X-rays with asymmetric Laue crystals. I. Theoretical considerations*. Journal of Applied Crystallography, 2001. **34**: p. 504-509.
12. *Pixium flat panel detector*. 2011; Available from: [http://www.thalesgroup.com/Portfolio/Security/Digital\\_detector\\_Pixium\\_RAD\\_4600\\_Portable\\_3543\\_3543C/?pid=1568](http://www.thalesgroup.com/Portfolio/Security/Digital_detector_Pixium_RAD_4600_Portable_3543_3543C/?pid=1568).
13. Daniels, J.E. and M. Drakopolous, *High-energy x-ray diffraction using the Pixium 4700 flat panel detector*. Journal of Synchrotron Radiation, 2009. **16**(4).

14. *Perkin Elmer, Large Area Flat Panel Detectors*. 2011; Available from: <http://www.perkinelmer.com/AU/pages/050/flat-panel-detectors/xrd-16-inch-field-of-view-detectors.xhtml>.
15. *ADSC Quantum detector*. 2011; Available from: <http://www.adsc-xray.com/products.html>.
16. *PCO Dimax CMOS camera*. 2011; Available from: <http://www.pco.de/high-speed-cameras/pcodimax/>.
17. Chapman, K.W., P.J. Chupas, and C.J. Kepert, *Direct Observation of a Transverse Vibrational Mechanism for Negative Thermal Expansion in Zn(CN)<sub>2</sub>: An Atomic Pair Distribution Function Analysis*. *Journal of the American Chemical Society*, 2005. **127**: p. 15630-15636.